Physiol Genomics 41: 244–253, 2010.
First published February 23, 2010; doi:10.1152/physiolgenomics.00020.2010.

Identifying genetic loci and spleen gene coexpression networks underlying immunophenotypes in BXD recombinant inbred mice

Rachel M. Lynch,[1] Sudhir Naswa,[2] Gary L. Rogers, Jr.,[2] Stephen A. Kania,[3] Suchita Das,[1] Elissa J. Chesler,[1,4] Arnold M. Saxton,[5] Michael A. Langston,[2] and Brynn H. Voy[1,5]

[1]*Systems Genetics Group, Oak Ridge National Laboratory, Oak Ridge; Departments of* [2]*Electrical Engineering and Computer Science and* [3]*Comparative Medicine, University of Tennessee, Knoxville, Tennessee;* [4]*The Jackson Laboratory, Bar Harbor, Maine; and* [5]*Department of Animal Science, University of Tennessee, Knoxville, Tennessee*

Submitted 12 January 2010; accepted in final form 22 February 2010

Lynch RM, Naswa S, Rogers GL Jr, Kania SA, Das S, Chesler EJ, Saxton AM, Langston MA, Voy BH. Identifying genetic loci and spleen gene coexpression networks underlying immunophenotypes in BXD recombinant inbred mice. *Physiol Genomics* 41: 244–253, 2010. First published February 23, 2010; doi:10.1152/physiolgenomics.00020.2010.—The immune system plays a pivotal role in the susceptibility to and progression of a variety of diseases. Due to a strong genetic basis, heritable differences in immune function may contribute to differential disease susceptibility between individuals. Genetic reference populations, such as the BXD (C57BL/6J × DBA/2J) panel of recombinant inbred (RI) mouse strains, provide unique models through which to integrate baseline phenotypes in healthy individuals with heritable risk for disease because of the ability to combine data collected from these populations across both multiple studies and time. We performed basic immunophenotyping (e.g., percentage of circulating B and T lymphocytes and $CD4^+$ and $CD8^+$ T cell subpopulations) in peripheral blood of healthy mice from 41 BXD RI strains to define the immunophenotypic variation in this strain panel and to characterize the genetic architecture that underlies these traits. Significant QTL models that explained the majority (50–77%) of phenotypic variance were derived for each trait and for the T:B cell and $CD4^+$:$CD8^+$ ratios. Combining QTL mapping with spleen gene expression data uncovered two quantitative trait transcripts, *Ptprk* and *Acp1*, as candidates for heritable differences in the relative abundance of helper and cytotoxic T cells. These data will be valuable in extracting genetic correlates of the immune system in the BXD panel. In addition, they will be a useful resource for prospective, phenotype-driven model selection to test hypotheses about differential disease or environmental susceptibility between individuals with baseline differences in the composition of the immune system.

quantitative trait loci; quantitative trait transcript; eQTL; CD4:CD8 ratio; T:B cell ratio; T lymphocytes; B lymphocytes; Ptprk; Acp1

SYSTEMS GENETICS TAKES a top-down approach to disease susceptibility by seeking to identify relationships between genetic variants, intermediate molecular, biochemical and cellular pathways, and overlying systems-level phenotypes from large-scale molecular and phenotypic analyses. Typically, putative interconnections are built through correlational analyses of diverse data types collected across genetically heterogeneous populations. These data are often obtained using genetic reference populations, i.e., populations that are genetically stable and thus reproducible, allowing data integration across time and from diverse studies and creating the possibility to uncover novel relationships among genes, pathways, and diseases. A number of genetic reference populations exist for mouse, the largest of which is the BXD (C57BL/6J × DBA/2J) recombinant inbred (RI) strain panel, consisting of 81 extant strains for which genotype data are publicly available (56). As the depth of phenotyping for a reference panel like the BXD strain set increases, so does the ability to interconnect physiological systems through genetic correlation of phenotypes. Such discoveries can be valuable for determining the molecular basis for a phenotype, for identifying biomarkers for disease processes, and for elucidating interconnections between apparently divergent physiological systems.

The burgeoning evidence that inflammation either initiates or fuels a wide variety of diseases and pathologies suggests that immune system components are likely to emerge in many systems-level networks of disease susceptibility. Disorders not traditionally linked with the immune system such as obesity and insulin resistance are now causally linked to inflammatory processes and mobilization of immune cells (36, 54, 78). While the abundance of specific lymphocyte subpopulations is altered by numerous environmental factors such as infection and diet (5, 73, 86), these traits are also under tight genetic control (2, 25, 41). The involvement of immune processes in myriad diseases, many of which have a genetic risk, coupled with a strong genetic basis for immune function, raises the possibility that genetic variation in immune phenotypes per se may contribute to differential disease susceptibility between individuals. Supportive of this concept is a recent report by Dendrou et al. (28), using the Cambridge BioResource, which is the human equivalent of a genetic reference population consisting of ~5,000 healthy, genotyped individuals living near Cambridge, UK, who agreed to be studied repeatedly over time. Dendrou and colleagues linked a specific T cell phenotype - relative expression of CD25 on the surface of $CD4^+$ memory T cells - with a haplotype previously shown to confer protection from type I diabetes. Understanding the genetic basis of specific immunophenotypes (IPs) may therefore be valuable in understanding susceptibilities and/or progression of diseases, such as multiple sclerosis and rheumatoid arthritis, which are characterized by dysregulation or imbalances of distinct immune cell populations (26, 35, 63, 68).

As a first step toward determining the heritable differences in IPs that may predict outcomes of disease and environmental exposures, we profiled the abundance of major lymphocyte subpopulations ($CD79^+$, $CD3^+$, $CD4^+$, and $CD8^+$) in peripheral blood of healthy, unperturbed mice from the BXD strain panel. These data were integrated with existing genotype data in quantitative trait loci (QTL) mapping to characterize the

Address for reprint requests and other correspondence: B. Voy, 201E McCord Hall, 2640 Morgan Circle Dr., Knoxville, TN 37996-4574 (e-mail: bhvoy@utk.edu).

Downloaded from http://physiolgenomics.physiology.org/ by 10.220.32.247 on October 21, 2016

genetic architecture that underlies these traits. They were further combined with microarray data we collected from spleens of the same strain panel to highlight potential candidate genes within significant QTL. Graph algorithms were used to identify gene expression networks that correlate with and are potential mediators of IPs, and are thus potential targets for environmental stimuli that act on the immune system Herein we present evidence that peripheral IPs are under significant genetic control in the BXD population and describe genes and coexpression networks linking genetic variation to immunophenotypic diversity.

METHODS

Animals. C57BL/6J, DBA/2J, and BXD RI stocks from *strains 6–42* were obtained from The Jackson Laboratory (Bar Harbor, ME). BXD RI stocks from *strains 43–100* were obtained from Dr. Lu Lu and Dr. Robert Williams from the University of Tennessee Health Science Center (UTHSC, Memphis, TN). BXD RI lines were housed and propagated in the specific pathogen-free (SPF) Russell Vivarium at Oak Ridge National Laboratory (ORNL). Mice received irradiated Purina Diet #5083 and chlorinated water ad libitum. The housing conditions were maintained at 70 ± 2°F and 40–60% humidity. A total of 45 BXD strains were used for spleen expression profiling, immunophenotyping, or both. This subset of the BXD panel was chosen from the set of strains maintained at ORNL based on consistent breeding performance and to represent a balanced combination of the original BXD strains developed at The Jackson Laboratory (71, 72) and the advanced intercross strains developed at the UTHSC (56). Between 10 and 12 wk of age, mice were killed by cervical dislocation and either blood was collected for immunophenotyping or the spleens were harvested for RNA expression profiling. All studies were approved by the Animal Care and Use Committee at Oak Ridge National Laboratory.

Immunophenotyping. Flow cytometry was used for the immunophenotyping of male and female mice (average of four mice/sex/strain) from 41 BXD strains and the parental strains. Blood was collected by retro-orbital sinus puncture into EDTA tubes, and red blood cells were lysed using lysis buffer (Sigma-Aldrich, St. Louis, MO). Following centrifugation, the white blood cell pellet was suspended in buffer (PBS, 0.2% sodium azide, 0.02% heat-inactivated FBS) and divided into four aliquots for each set of monoclonal antibodies and a blank negative control. Lymphocytes were stained with the appropriate antibody or antibodies for 45 min at 4°C. The negative control was incubated with PBS. One tube was dual-stained with anti-CD3 (PE, clone 17A2) and anti-CD79b (FITC, clone HM79b). Another tube was dual-stained with anti-CD4 (PE, clone H129.19) and anti-CD8a (FITC, clone 53-6.7). The remaining tube was stained with anti-MHC class II (R-PE, clone NIMR-4). Antibodies were purchased from BD Biosciences (Franklin Lakes, NJ), except MHC class II-RPE, which was purchased from Southern Biotech (Birmingham, AL). Following incubation, the samples were centrifuged and suspended in PBS. All samples were stored on ice in the dark until analyzed by flow cytometry. At least 10,000 cells per sample were analyzed using a Beckman Coulter Epics XL flow cytometer (Brea, CA). Data were analyzed using EXPO32 ADC Software (Beckman Coulter). Lymphocytes were gated for analysis based on forward and side scattering profiles. The IPs measured included the proportion of circulating T cells (%CD3), B cells (%CD79), $CD4^+$ T cells (%CD4), $CD8^+$ T cells (%CD8), as well as the median expression of major histocompatibility complex II (MHCII median) on $MHCII^+$ lymphocytes (%MHCII).

Identification of immunophenotype QTL. Flow cytometric data were analyzed for quality based on efficient staining of lymphocytes and within-individual consistency (e.g., %CD79 approximately equaling %MHCII and sum of %CD4 plus %CD8 approximately equaling %CD3). Only high-quality immunophenotype data were used for further analysis, resulting in an average of 3.3 males and 3.2 females per strain for each IP. T cell to B cell ratio, $CD4^+$ to $CD8^+$ ratio, and MHC II median fluorescence were normalized using natural log transformation (i.e., LN T:B, LN CD4:CD8, LN MHCII).

QTL analysis was performed using genotype data obtained from GeneNetwork (http://www.genenetwork.org/dbdoc/BXDGeno.html). This database contains nearly 3,800 informative single-nucleotide polymorphisms (SNPs) and microsatellite markers originally reported by Shifman et al. (62) that have been re-aligned with National Center for Biotechnology Information (NCBI) Build 36. QTL for each IP were identified using the QTL package (16) in R (http://www.r-project.org). The multiple imputation method of Sen and Churchill (60) was used to perform single-QTL genome-wide scans. Genome-wide significance thresholds were calculated based on 1,000 permutations (24). The cut-off P values for significant and suggestive loci were $P = 0.05$ and $P = 0.63$, respectively (42).The ± 1 logarithm of the odds ratio (LOD) support intervals for each QTL were calculated using the lodint function in R/QTL. Multiple-QTL modeling was performed using stepwise linear regression in SAS (SAS Institute, Cary, NC); a P value of 0.05 was used as the threshold for terms to remain in the final model.

Expression profiling. Transcriptome profiling was performed in spleens from an independent set of mice representing 38 BXD strains (34 of which were immunophenotyped). Total spleen RNA was isolated from spleens stabilized in RNAlater (Sigma-Aldrich) using RNeasy Mini Kits (Qiagen, Valencia, CA). RNA concentration and quality were assessed using Experion RNA StdSens Chips on the Experion system (Bio-Rad, Hercules, CA). Each BXD sample profiled consisted of a pool of equal amounts of RNA from either two males or two females per strain. Expression profiling was performed by Genome Quebec (Montreal, Canada) using the Mouse WG-6 v1.1 BeadChip on the Illumina platform (San Diego, CA). Six strains were analyzed per chip. The data were normalized using variance stabilizing transformation followed by robust spline normalization using the R/lumi package (30) in Bioconductor (32). Raw and normalized microarray data have been uploaded to NCBI's Gene Expression Omnibus database (http://www.ncbi.nlm.nih.gov/projects/geo; accession GSE19935) according to MIAME standards (14). Expression data, along with all IP data, are also available through GeneNetwork (http://www.genenetwork.org).

Transcriptome map and expression QTL analysis. Of the 34,492 probes on the Illumina arrays, 11,445 transcripts demonstrated variable expression across the panel (coefficient of variation >0.01) and were used for expression QTL (eQTL) analysis. QTL Reaper (http://www.genenetwork.org/qtlreaper.html) was used to identify the maximum likelihood ratio statistic and a permuted P value (1,000 permutations) for each transcript. QTL Reaper performs Haley-Knott regression for QTL analysis, with an adaptive permutation by transcript that runs an increased number of permutations for those traits with significant results to ensure precise P value estimation at the low end of the P distribution. This method is fast and sufficient for high-density marker maps as are available for the BXD RI lines. At a P value threshold of 0.05 over the entire array, 1,881 transcripts were associated with 686 loci. These eQTLs were classified as *cis* or *trans* according to their genomic positions (located within or beyond 10 Mb of transcription start site, respectively). Permutation testing was used to define the maximum number of transcripts likely to be associated by chance in *trans* with an eQTL. The 1,881 transcripts were randomly assigned to the 686 significant loci; in 10 million permutations, the maximum number of transcripts associated in *trans* with a single marker was 19. Therefore, we analyzed only the *trans*-eQTL bands in which a single marker was associated with 20 or more transcripts.

Statistical modeling and graph algorithms. MGI (http://www.informatics.jax.org) was used to extract genes located within the ± 1 LOD support intervals for the two significant QTLs identified for the CD4:CD8 immunophenotype. Stepwise linear regression in SAS was

Downloaded from http://physiolgenomics.physiology.org/ by 10.220.32.247 on October 21, 2016

used to model the CD4:CD8 ratio using the expression of these genes. Graph algorithms were performed as described previously (76), and all source codes are available from the authors. Graphs were created from microarray data by computing all pair-wise Pearson correlations between expressed transcripts and then filtering the matrix to retain only statistically significant correlations based on a false discovery rate of 5% (q-value <0.05, Ref. 67). Maximal cliques were extracted and anchored cliques identified as previously described (76). A bipartite graph was created with one partition being the expressed transcripts and the second partition being a set of five IPs (CD3%, LN T:B, CD4%, CD8%, LN CD4:CD8). Pearson correlations were computed between each possible pairing of transcript expression and immunophenotype. Edges in the bipartite graph were filtered to retain correlations of interest ($P < 0.001$), and maximal bicliques were then extracted. Gene ontology (GO) enrichment analysis was performed using DAVID (37); Benjamini-Hochberg false discovery rate-corrected P values are reported (8).

RESULTS

We began by profiling a panel of IPs in male and female C57BL/6J and DBA/2J mice to define baseline differences in the two BXD parental strains. Peripheral blood was analyzed for proportion of circulating T cells ($CD3^+$), B cells ($CD79^+$), T helper cells ($CD4^+$), cytotoxic T cells ($CD8^+$), and expression of major histocompatibility complex II (MHCII) on $MHCII^+$ lymphocytes using flow cytometry. As shown in Table 1, the parental strains differ significantly in each of these traits ($P < 0.05$) except for $CD3^+$ cells ($P = 0.184$) and $CD8^+$ T cells ($P = 0.064$). C57BL/6J mice demonstrate a higher percentage of circulating B cells and $CD8^+$ T cells and lower levels of $CD4^+$ T cells compared with DBA/2J mice, which is consistent with previous reports (21, 52, 74).

The same panel of IPs was profiled across a set of 41 BXD strains to establish the immunophenotypic diversity in this RI panel and to model the genetic regulation of each trait. ANOVA indicated a significant effect of strain on each IP ($P < 0.0001$), manifested as broad ranges for each of the traits across the strains. For example, the percentage of T lymphocytes varies over fivefold (10.3–56.1%), while the percentages of $CD4^+$ and $CD8^+$ lymphocytes vary over sixfold (5.6–35.6 and 4.4–26.4%, respectively) (Fig. 1, Supplemental Table S1).[1] These ranges relative to those of the parentals illustrate the genetic complexity of the traits and are within the range of the phenotypic diversity found in a survey of 32 standard inbred strains of diverse origin (10, 57). There is also a significant strain*sex interaction effect for each immunophenotype ($P < 0.05$), but the effect is much smaller (F statistic < 30%) than that of the main strain effects. Thus, overall strain effects were modeled for each immunophenotype.

QTL analysis was performed on each IP as well as the T:B and CD4:CD8 ratios to identify overlapping and unique loci associated with each trait. We began with MHC II density as a reference trait with a defined genetic basis on Chromosome (Chr) 17, a region in which the BXD parental strains carry different haplotypes (C57BL/6J carries the H-2^b haplotype and DBA/2J carries the H-2^d). Not surprisingly, the genotype at the H2 locus is the largest factor in explaining median expression of MHCII on MHCII-expressing lymphocytes (Supplemental Fig. S1A). The locus itself accounts for 57% of the variance within the BXD panel (LOD = 7.52, $P < 0.001$), with the DBA/2J genotype increasing MHCII expression. A suggestive secondary locus, Chr 10 @ 114Mb, accounts for an additional 4.5% of the variance. The genetic basis for variation in the remaining IPs was modeled by first performing single model genome-wide scans (Supplemental Fig. S1) and then using suggestive and significant loci from those scans in multilocus regression to allow for additive and interactive contributions of multiple loci. A 9 Mb region on Chr 17 spanning the H2 locus was identified as either suggestive or significant for single model scans of each trait except for the CD4:CD8 ratio (Fig. 2). The majority of variance (50.1–77.5%) for each trait is explained by models incorporating the Chr 17 region in combination with at most three additional loci (Table 2). T and B cells were measured as a percentage of total gated lymphocytes and collectively represent the majority of this population, making these two measurements highly inversely correlated. Accordingly, the QTL models for each trait are very similar. The relative abundance between these two cell types (natural log transformed T:B ratio, or LN T:B) was mapped to identify loci that may be involved in lymphocyte maturation. The T:B phenotype is partially explained by interactions between loci on Chrs 3 and 7 and between the Chr 3 locus and H2 locus. In combination with the additive effects of the H2 locus and an additional region on Chr 11, this model explains 77.5% of the variation in the T:B ratio. The only locus important in modeling the T:B ratio that was not identified for either lymphocyte population separately (i.e., %CD3 and %CD79) is the locus on Chr 7. The complete set of significant and suggestive QTLs for each immunophenotype is depicted in Fig. 2.

Genetic control of T cell abundance was further probed by mapping loci that contribute to variance in the major T cell subpopulations, $CD4^+$ and $CD8^+$ T cells. While QTL analysis identified the H2 locus as contributing to both %CD4 and %CD8 (LOD of 4.07 and 3.79, respectively), the remaining QTLs were unique to the particular T cell subpopulations (Fig. 2). A multilocus model consisting of three loci (on Chrs 10, 12, and the H2 locus) explains 50.1% of the variance in %CD4, while a model consisting of a locus on Chr 3 with the H2 locus explains 56.6% of the variance in %CD8. The ratio of $CD4^+$ to $CD8^+$ cells was used in QTL analysis after normalization using natural log transformation (LN CD4:CD8). Two loci (Chr 10 @ 31Mb, LOD = 4.24 and Chr 12 @ 31Mb, LOD = 4.28) were identified as significant, independent contributors to this trait (Supplemental Fig. S1C, Table 2). At both loci, the DBA/2J allele shifts the ratio in favor of $CD4^+$ cells, consistent

[1] The online version of this article contains supplemental material.

Table 1. *Differences in peripheral blood immunophenotypes in C57BL/6J and DBA/2J mice*

Immunophenotype	C57BL/6J Mean	DBA/2J Mean	P Value
% CD3 lymphocytes	32.06 ± 1.03	35.60 ± 2.21	0.1840
% CD79 lymphocytes	61.40 ± 0.98	53.86 ± 2.73	0.0352*
LN T:B	−0.65 ± 0.03	−0.42 ± 0.09	0.0392*
% CD4 lymphocytes	23.84 ± 1.64	31.56 ± 2.41	0.0190*
% CD8 lymphocytes	7.98 ± 0.56	6.50 ± 0.47	0.0636
LN CD4:CD8	1.10 ± 0.10	1.58 ± 0.07	0.0012†
% MHCII lymphocytes	61.62 ± 1.87	51.22 ± 2.64	0.0194*
LN MHCII density	3.53 ± 0.16	4.31 ± 0.08	0.0003†

Data shown as means ± SE of 5–9 mice per strain. P value indicates significance of strain effect (*$P < 0.05$, †$P < 0.01$).

Downloaded from http://physiolgenomics.physiology.org/ by 10.220.32.247 on October 21, 2016

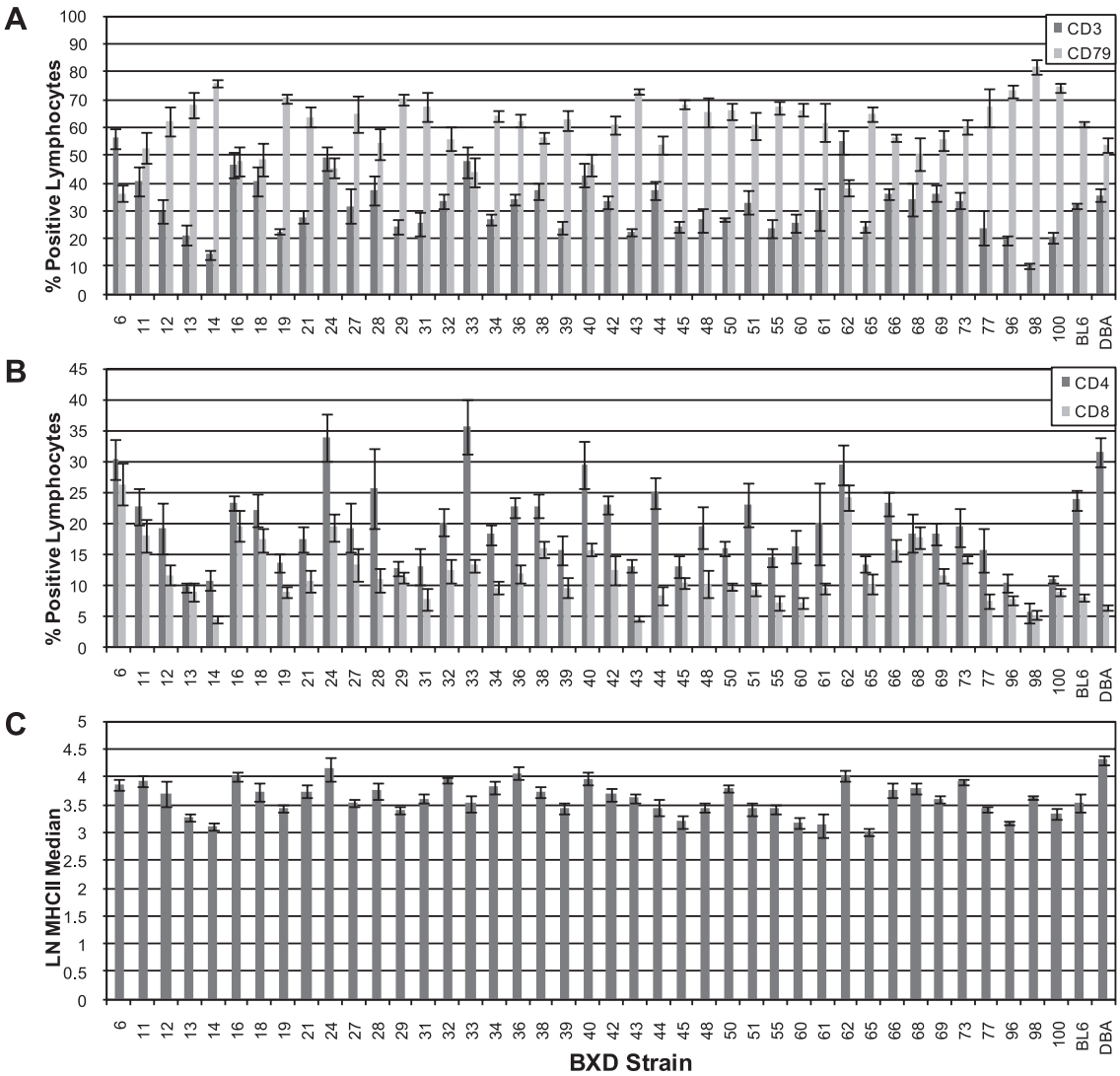

Fig. 1. Peripheral blood lymphocyte subpopulations of BXD and parental strains: %CD3 and %CD79 lymphocytes (*A*), %CD4 and %CD8 lymphocytes (*B*), and MHCII density on MHCII$^+$ lymphocytes (LN of median MHCII fluorescence, *C*). Data shown as means ± SE of at least 3 males and 3 females per strain.

with the increased abundance of CD4$^+$ cells in the DBA/2J parents (Table 1). These two loci explain nearly 54% of the variation in the CD4:CD8 ratio. Interestingly, neither region is implicated in control of either T cell subtype as analyzed independently, suggesting that these two regions contain genetic variation that contributes to a differentiation process in which one cell type is retained at the expense of the other.

eQTL profiling has emerged as a means to identify loci linked directly or indirectly to regulation of gene expression (15, 29, 38, 59). We performed eQTL mapping using spleen microarray data to determine whether the QTL regions identified for IP traits also harbored *trans*-eQTL bands, loci that are linked to expression of multiple genes and could thus be implicated in mechanistic control of the trait(s) through coordinated transcriptional regulation. Spleen was chosen because it contains abundant levels of both B and T lymphocytes and contributes to multiple aspects of immune function. Two *trans*-bands exceeded the maximal size of 18 transcripts obtained by permutation testing, consisting of 42 and 30 transcripts located on Chrs 4 (@ 139.0 Mb) and 12 (@ 15.8 Mb), respectively (Supplemental Fig. S2). Neither *trans*-band colocalized with IP QTLs, nor were the transcripts associated with each *trans*-band enriched for functions suggestive of IP regulation. Both bands did, however, contain an abundance of genes involved in cell cycle, cell division and DNA replication, which may have general relevance for heritable regulation of gene expression in the BXD panel.

We further exploited the microarray data to identify potential IP candidate genes by determining if expression of one or more genes within the QTL intervals were correlated with the overlying trait(s), a strategy that has been used successfully for other traits (7, 45, 55). We identified quantitative trait transcripts (QTTs), transcripts whose expression is correlated with a phenotype (55), for the T:B and CD4:CD8 ratios. We focused on these two traits because they capture relative abundance of multiple cell types and have significant QTLs. Pearson's correlation coefficients were calculated between expression levels of genes residing within the ± 1 LOD support intervals for each QTL and the immunophenotype data. Of the 517 genes located within these intervals for T:B ratio, 88 showed signif-

Downloaded from http://physiolgenomics.physiology.org/ by 10.220.32.247 on October 21, 2016

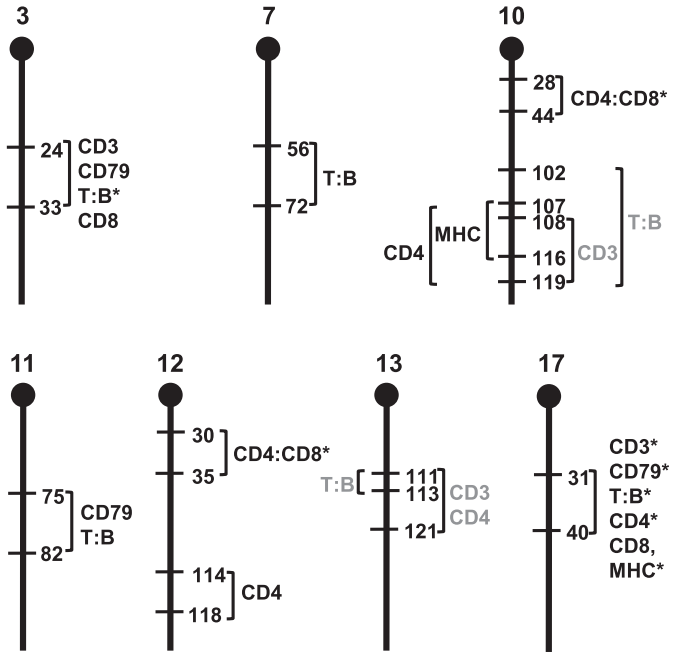

Fig. 2. Summary of BXD immunophenotype (IP) quantitative trait loci (QTLs). The ranges indicate the ± 1 logarithm of the odds ratio (LOD) support intervals for each significant and suggestive QTL, in Mb. IPs are %CD3 lymphocytes (CD3), %CD79 lymphocytes (CD79), LN of CD3:CD79 (T:B), %CD4 lymphocytes (CD4), %CD8 lymphocytes (CD8), LN of CD4:CD8 (CD4:CD8), and LN of MHCII median expression on MHCII$^+$ lymphocytes (MHC). *Significant QTL ($P < 0.05$) in single-locus genome-wide scan. IP labels in black are QTLs that are significant in the final model ($P < 0.05$); gray IP labels are not significant in final model.

icant correlation with the phenotype ($P < 0.05$). Gene Ontology (GO) enrichment analysis indicated that this set of genes was significantly enriched in processes related to antigen presentation and processing, as expected from the fact that many of these genes lie within the H2 locus on Chr 17. This set also contains a small number of genes (30 genes) that are highly correlated with T:B but reside on other chromosomes, the strongest of which are mitofusin 1 (r = 0.626, $P < 0.0001$) and phospholipase D1 (r = −0.563, $P = 0.0005$), both of which are within the QTL on Chr 3. Mitofusins are mitochondrial fusion proteins that have recently been linked to the innate antiviral defense system (82). Phospholipase D1 was shown to be critical for coordination of inflammatory signaling through TNF-α in leukocytes (61).

Similar analysis of the QTL regions for the CD4:CD8 phenotype highlights a smaller set of potential candidate genes for this trait in the BXD panel. Of the 115 genes located within the QTL intervals for CD4:CD8 ratio, only 9 (7.8%) were significantly correlated with the CD4:CD8 phenotype. Of these, the most highly correlated QTT (r = 0.575; $P = 0.0004$) is the transcript for protein tyrosine phosphatase, receptor type, K (*Ptprk*), a phosphatase expressed in spleen and other tissues (81) . Loss of *Ptprk* due to a spontaneous deletion in Long Evans Cinnamon (LEC) rats was recently shown to underlie the deficiency in CD4$^+$ T cells in this model (40). Conversely, our data link increased expression of *Ptprk* with elevated levels of CD4$^+$ cells. Stepwise linear regression of *Ptprk* and the eight other QTL interval genes correlated with the CD4:CD8 ratio was used to estimate the amount of trait variance explained by expression of these genes. A model containing *Ptprk* along with acid phosphatase 1 (*Acp1*; also known as low molecular weight protein tyrosine phosphatase) and laminin B-1 (*Lamb1–1*) explains 61% of variance in the CD4:CD8 phenotype ($P < 0.0001$). Like *Ptprk*, *Acp1* is also a strong candidate gene for heritable variation in CD4:CD8 in the BXD panel. Polymorphisms in the human ACP1 gene have been correlated with susceptibility to a number of inflammatory and autoimmune disorders such as type I diabetes, allergy, and atherosclerosis, all disorders in which CD4 and/or CD8 cells are implicated in pathogenesis (9, 18, 49). *Lamb1–1* has not been linked specifically to immune function but is widely expressed in spleen (46).

Table 2. *Summary of final QTL models for BXD immunophenotypes*

Immunophenotype	Final Model	Variance Explained, %	QTLs				
				Marker	Chr	Position, Mb	LOD
%CD3	Loc1*2 + Loc2	58.9	Loc1	rs13477026	3	27	3.72*
			Loc2	rs13482963	17	35	5.28*
%CD79	Loc1 + Loc2 + Loc3	67.2	Loc1	rs13477026	3	27	4.17*
			Loc2	rs13481119	11	79	2.54
			Loc3	rs13482947	17	31	5.41*
LN T:B	Loc1*2 + Loc1*4 + Loc3+ Loc4	77.5	Loc1	rs13477026	3	27	3.81
			Loc2	rs13479274	7	58	2.64
			Loc3	rs13481119	11	79	2.61
			Loc4	rs13482947	17	31	5.62*
%CD4	Loc1*2 + Loc3	50.1	Loc1	rs3690259	10	114	3.10
			Loc2	rs3694890	12	118	2.70
			Loc3	rs13482963	17	35	4.07*
%CD8	Loc1*2 + Loc2	56.6	Loc1	rs13477030	3	28	3.82*
			Loc2	rs3672987	17	33	3.79*
LN CD4:CD8	Loc1 + Loc2	53.8	Loc1	rs13480570	10	31	4.24*
			Loc2	rs6225272	12	31	4.28*
LN MHC median	Loc1 + Loc2	61.5	Loc1	rs3690259	10	114	2.81
			Loc2	rs13482947	17	31	7.52*

Models were analyzed using significant and suggestive quantitative trait loci (QTLs) from single locus genome-wide scans. Representative single nucleotide polymorphism markers for each locus in the final models are reported; genome locations are according to NCBI Build 36. LOD, logarithm of odds scores based on single locus models. *Significant QTLs; all others are suggestive.

Downloaded from http://physiolgenomics.physiology.org/ by 10.220.32.247 on October 21, 2016

Our group has developed a number of graph algorithms based on the extraction of cliques and other dense subgraphs to identify putative gene coexpression networks from large-scale omics data (6, 11, 22, 43, 76, 84). Here we use the concept of anchored clique to extract networks of genes coexpressed with *Acp1* and *Ptprk* that may provide insight into the mechanisms linking each gene to the CD4:CD8 phenotype. Both genes encode phosphatases and have been linked through genetic association studies to a number of inflammatory conditions, but relatively little is known about the cellular pathways in which each gene functions. The largest clique containing *Acp1* in a graph thresholded at q-value = 0.05 (with corresponding P = 0.0026) consisted of a total of 500 transcripts. The correlations of genes within this clique range from |r| = 0.550 to 0.917. GO enrichment revealed that this *Acp1* coexpression network is highly enriched for genes involved in cell cycle (P = 2.0e-22, Benjamini = 1.1e-18), cell division (P = 1.6e-20, Benjamini = 4.2e-17), and DNA replication (P = 2.4e-18, Benjamini = 3.2e-15). To insure that this high degree of GO enrichment was not somehow an artifact of our specific dataset, we identified genetic correlates of *Acp1* expression in an independent spleen array dataset from 24 BXD strains within GeneNetwork (27). As with our data, *Acp1* expression was highly significantly correlated with genes involved in cell cycle and related processes (e.g., GO term M phase, Benjamini = 1.13e-18). The cell cycle enrichment in our *Acp1* anchored clique is also represented in the KEGG pathway for cell cycle control (P = 3.3e-12, Benjamini = 6.5e-10). Interestingly, of the 20 genes included in the KEGG pathway and coexpressed with *Acp1*, 18 are regulated by phosphorylation. These results suggest that abundance of the *Acp1* transcript per se may regulate phosphorylation status of cell cycle targets, either directly or indirectly, in the spleen. Similar analysis was performed for the maximal anchored clique of 135 genes containing *Ptprk*, but significant GO enrichment was not observed.

One of our long-term interests is to identify gene coexpression networks linked to immune function in healthy individuals and to determine how these networks are perturbed by environmental factors that promote inflammation and/or alter immune function. To visualize the intersection between gene networks associated with IPs, we used a biclique algorithm to identify the largest set of transcripts in which each member is significantly correlated with each other and one or more phenotypes. Pearson correlations were computed between each transcript and five immunophenotype measurements (%CD4, %CD3, LN T:B, %CD8, and LN CD4:CD8), and the matrix was thresholded to retain only those correlations most likely to symbolize true relationships ($P < 0.001$), leaving a total of 218 transcripts that are significantly correlated with one or more IPs. The relationship between gene expression and IPs are represented in Fig. 3, and as expected significant overlap exists between the sets of genes associated with each trait. The members of each biclique are listed in Supplemental Table S2. For example, *Notch4* is correlated with %CD3, LN T:B, %CD4, and %CD8. *Notch4* is part of the highly conserved Notch family which play important roles in lymphocyte lineage commitment (70) and other cell-fate decisions (3). Specifically, there is evidence to support the role of *Notch4* in the differentiation and expansion of hematopoietic stem cells and in lymphomogenesis (75, 83). These data provide a starting point from which to test the impact of specific environmental variables on networks of genes linked to IPs of interest.

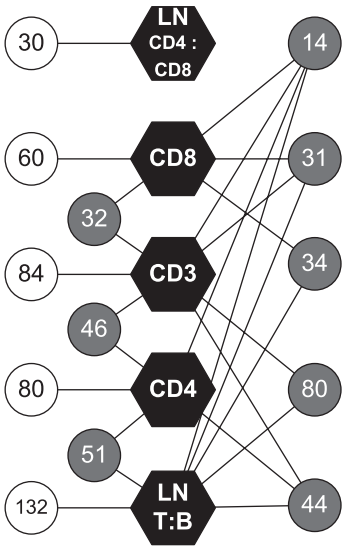

Fig. 3. Bipartite graph demonstrating the connectivity of 5 IPs and transcript expression. IPs are listed in the center of the graph and are symbolized by hexagons. The numbers of transcripts correlated ($P < 0.001$) with the IP(s) are depicted in the circles. The transcript sets symbolized by white circles create a maximal biclique with a single IP, while the transcript sets that create a maximal biclique with >1 IP are symbolized with gray circles. The transcripts included in each biclique are listed in Table S2.

DISCUSSION

Systems genetics enables the detection of QTLs and the identification of putative candidate genes for further testing and validation. In parallel, it produces phenomic data that can be mined in the context of the system by integrating it with all of the other multiscale and diverse data types obtained from the same population. At a total of 79 strains, the BXD RI strain panel is the largest inbred mouse RI panel, and one for which an abundance of genomic resources now exist (56). We characterized the range of variation and the genetic architecture of IPs in the BXD RI panel to produce a baseline profile of the immune system that can be integrated into systems genetics studies with this population. These data are relevant for genetic susceptibility to the plethora of environmental factors and disorders that invoke the immune system, e.g., ionizing radiation exposure and diet-induced obesity.

We found that genetic models explain the majority of variation in each of the IPs, which is consistent with reports from humans and other species that lymphocyte subpopulations in healthy individuals are under strong genetic control. Three of the IPs (proportions of B, $CD4^+$ and $CD8^+$ lymphocytes in peripheral blood) were previously profiled in 22 of the same BXD lines included in our study (21). Two of the three IPs are significantly correlated with our data (%B lymphocytes, r^2 = 0.530, P = 0.010; %CD8 lymphocytes, r^2 = 0.437, P = 0.041) despite the passage of several years between studies and the use of independent BXD breeding colonies and institutions, highlighting the genetic stability of these phenotypes. The QTLs identified for these three traits differ between the two studies, likely because the Chen and Harrison (21) study relied on 35 BXD strains from the original BXD panel (*strains 1–42*)

Downloaded from http://physiolgenomics.physiology.org/ by 10.220.32.247 on October 21, 2016

and a limited number of genetic markers, while ours was balanced between the original BXD set and the advanced recombinant inbred set produced by Peirce et al. (56). Recent polymorphisms in this population (62) have been shown to influence the location and direction of QTL effects in these populations (58). In addition, a significant increase in the number of informative genetic markers are now available for the BXD panel and were used herein, which also may contribute to the discrepancy in QTL positions. Our reported QTL intervals (and those for many other traits mapped using the BXD panel) will likely be further refined with upcoming availability of genotype data across a panel of 580,000 SNPs, data that will soon be available through the GeneNetwork website (R. W. Williams, personal communication).

Identifying QTLs is relatively straightforward and rapid when using genetic reference panels such as BXD for which genotype data are readily available; cloning the causative polymorphism and confirming its role in phenotypic determination is a much more elusive target and one that we have not attempted. However, by combining QTL mapping with gene expression data, we have winnowed the list of potential candidate genes for traits of interest to a manageable number for further study. This approach produced two particularly compelling candidate genes - *Ptprk* and *Acp1* - within the two significant QTLs associated with CD4:CD8, a trait used clinically as a marker for the prognosis of human immunodeficiency virus (HIV) (47), rheumatoid arthritis (31), and other diseases. *Ptprk* encodes a receptor-type protein-tyrosine phosphatase with no specific properties that link it to lymphocyte development. However, a potential role for Ptprk in $CD4^+$ T cell development was serendipitously uncovered in studies of the LEC rat, a model of Wilson's disease (due to a mutation in the copper transporting ATPase gene) that also had been noted to be deficient in $CD4^+$ T cells (1). Recently, two groups (4, 40) used linkage analysis to identify a deletion containing *Ptprk* in LEC rats and confirmed that loss of Ptprk is responsible for defective $CD4^+$ T cell development. Clinically, deletions of the chromosomal region containing PTPRK (chromosome 6q22–23) are frequently present in high-grade non-Hodgkin's lymphoma (53, 85), and loss of this region is also predictive of poor prognosis in CNS lymphoma (20), implicating this phosphatase in oncogenesis of the immune system. We used coexpression analysis in an attempt to gain insight into Ptprk function in spleen, based on the concept of genetic correlation. However, many of the transcripts with which *Ptprk* is most tightly coexpressed are un- or poorly annotated, and no specific functions showed statistical enrichment. On the other hand, *Acp1*, the second candidate gene of interest for the CD4:CD8 phenotype, is part of a large clique of 500 transcripts that is highly enriched in functions related to cell cycle. *Acp1*, also known as low molecular weight protein tyrosine phosphatase, regulates phosphorylation status of a number of proliferative signaling molecules (64) and is upregulated in several types of cancers (48, 50). Genetic screens in humans link polymorphisms in or near the ACP1 locus to a variety of inflammatory diseases including allergy, asthma, and obesity (12), and Acp1 is involved in activation, adhesion, and differentiation of T cells (13, 33). The QTLs containing *Acp1* and *Ptprk* reside on separate chromosomes that showed significant independent and additive linkage with the CD4:CD8 phenotype, suggesting that genes within each locus may interact to affect CD4:CD8 ratio. At the molecular level Ptprk positively regulates the protein tyrosine kinase Src (77), which in turn phosphorylates and activates Acp1 (17, 69). Whether these events occur in the same cell type, and in one relevant to T cell development, is unknown but is worthy of further experimentation. It is worth noting that both Acp1 and Ptprk have been linked through genetic screens to colon cancer susceptibility (65, 66). Germane to our overarching interest in radiation sensitivity is the fact that both Acp1 and Ptprk have been shown to be altered by radiation exposure (34, 79).

Although Ptprk and Acp1 emerge as attractive candidates for the CD4:CD8 phenotype, a potential limitation of our study is that the tissue (spleen) used to highlight these QTTs is not the site of T lymphocyte lineage commitment and selection, processes thought to primarily occur within the thymus (19). However, it has been suggested that there are compensatory adjustments that occur within peripheral immune organs (i.e., spleen and lymph nodes) and alters the T cell peripheral population (52). Therefore, it is possible that the expression levels of *Ptprk* and *Acp1* in the thymus and spleen are regulated through similar mechanisms, or that the genetic polymorphisms that cause variation between strains exert similar effects in both tissues. If so, the relationship between trait values and expression levels would be predicted, even though the specific tissue profiled is not the primary tissue involved in the process of interest. Alternatively, the causative polymorphisms within the QTL intervals, whether in *Ptprk* and *Acp1* or other genes or regulatory elements, may act on processes that occur in the periphery, such as T cell proliferation. However, the mice used in this study were not exposed to any known immune challenges and were maintained in an SPF facility, and we would expect peripheral proliferation of T cells to be minimal in these animals. It is also possible that, despite convergent evidence to support their contribution to CD4:CD8, the causative polymorphism for variation in this trait do not act through either Acp1 or Ptprk.

Genetic correlations between IPs in the BXD panel and disease susceptibility would be enriched by more detailed characterization of T cell subpopulations beyond the classification as either Th ($CD4^+$) or Tc ($CD8^+$). For example, additional surface markers could be used to further classify $CD4^+$ cells as Th1, Th2, Th17, regulatory T (Treg), follicular helper T (Tfh), $\gamma\delta$ T cells, etc. Each of these cell types play important roles in host defense and autoimmune diseases, and understanding the genetic basis of T cell subpopulation distributions would be invaluable in elucidating susceptibilities to T cell-mediated disorders, such as rheumatoid arthritis (39, 44, 80).

One of the advantages of using BXD strains as a reference population is the wealth of genotypic, phenotypic, and gene expression information available for the panel, much of which is freely available through the online database GeneNetwork. For example, we transiently uploaded our data into GeneNetwork to scan for genetic correlation between our IPs and other traits measured on the BXD population. This ad hoc analysis revealed an association between the baseline T:B ratio profiled in our study and outcomes of *Chlamydia psittaci* exposure as measured by Miyairi and colleagues (51). Among BXD strains that persisted 30 days postinfection, both spleen weight and pathogen load in spleen (GeneNetwork records 11025 and 11026) are significantly correlated ($r = -0.811$, $P < 0.001$, and $r = -0.728$, $P = 0.003$, respectively) with the T:B

Downloaded from http://physiolgenomics.physiology.org/ by 10.220.32.247 on October 21, 2016

phenotype. The opportunity for such integrative analyses provided by the use of genetic reference populations such as the BXD panel highlights the strengths of systems genetics, namely the ability to assimilate genetic susceptibility to disease or the environment in the context of the healthy state through the stable genetic basis of the population. As the BXD strain continues to be phenotyped, the ability to connect seemingly disparate phenotypes grows proportionally. The Collaborative Cross, an idealized genetic reference population, should also be widely available within the next few years for expanded systems genetics studies (23).

In summary, we have characterized the genetic architecture of a set of basic but informative IPs in the BXD panel. We have uncovered potential candidate genes that contribute to genetic variation in the relative abundance of helper and cytotoxic T cells, and follow-on studies to test the roles of both Ptprk and Acp1 can now be initiated. Beyond the classical follow-ups to QTL mapping, these data can be a useful resource in choosing BXD strains with a particular baseline immunoprofile for the study of a particular disease susceptibility or progression. For example, we have gene expression data from spleen suggesting that low-dose radiation exposure differentially impacts T cell subpopulations in a way that depends on genetic background (R. L. Lynch, S. Das, A. M. Saxton, M. A. Langston, B. H. Voy, unpublished data). We can now use these BXD data to select strain subsets based on differences in T cell subpopulations and prospectively test if heritable differences in IPs alter radiation effects on immune function.

ACKNOWLEDGMENTS

We thank K. T. Cain for breeding the BXD mice at ORNL, Ginger D. Shaw for collecting blood and spleen samples, Vivek M. Philip for assistance with QTL mapping, and Dianne J. Trent for immunophenotyping.

GRANTS

The project was supported by the Low Dose Radiation Research Program of the Office of Biological and Environmental Research, Office of Science, Department of Energy ERKP650 and ERKP804.

DISCLOSURES

No conflicts of interest are declared by the authors.

REFERENCES

1. **Agui T, Oka M, Yamada T, Sakai T, Izumi K, Ishida Y, Himeno K, Matsumoto K.** Maturational arrest from CD4+8+ to CD4+8- thymocytes in a mutant strain (LEC) of rat. *J Exp Med* 172: 1615–1624, 1990.
2. **Amadori A, Zamarchi R, De Silvestro G, Forza G, Cavatton G, Danieli GA, Clementi M, Chieco-Bianchi L.** Genetic control of the CD4/CD8 T-cell ratio in humans. *Nat Med* 1: 1279–1283, 1995.
3. **Artavanis-Tsakonas S, Matsuno K, Fortini ME.** Notch signaling. *Science* 268: 225–232, 1995.
4. **Asano A, Tsubomatsu K, Jung CG, Sasaki N, Agui T.** A deletion mutation of the protein tyrosine phosphatase kappa (Ptprk) gene is responsible for T-helper immunodeficiency (thid) in the LEC rat. *Mamm Genome* 18: 779–786, 2007.
5. **Babcock GF, Taylor AF, Hynd BA, Sramkoski RM, Alexander JW.** Flow cytometric analysis of lymphocyte subset phenotypes comparing normal children and adults. *Diagn Clin Immunol* 5: 175–179, 1987.
6. **Baldwin NE, Chesler EJ, Kirov S, Langston MA, Snoddy JR, Williams RW, Zhang B.** Computational, integrative, and comparative methods for the elucidation of genetic coexpression networks. *J Biomed Biotechnol* 2005: 172–180, 2005.
7. **Bao L, Peirce JL, Zhou M, Li H, Goldowitz D, Williams RW, Lu L, Cui Y.** An integrative genomics strategy for systematic characterization of genetic loci modulating phenotypes. *Hum Mol Genet* 16: 1381–1390, 2007.
8. **Benjamini Y, Hochberg Y.** Controlling the false discovery rate - a practical and powerful approach to multiple testing. *J Roy Stat Soc Ser B-Method* 57: 289–300, 1995.
9. **Betts RJ, Kemeny DM.** CD8+ T cells in asthma: friend or foe? *Pharmacol Ther* 121: 123–131, 2009.
10. **Bogue MA, Grubb SC, Maddatu TP, Bult CJ.** Mouse Phenome Database (MPD). *Nucleic Acids Res* 35: D643–649, 2007.
11. **Borate BR, Chesler EJ, Langston MA, Saxton AM, Voy BH.** Comparison of threshold selection methods for microarray gene co-expression matrices. *BMC Res Notes* 2: 240, 2009.
12. **Bottini N, Bottini E, Gloria-Bottini F, Mustelin T.** Low-molecular-weight protein tyrosine phosphatase and human disease: in search of biochemical mechanisms. *Arch Immunol Ther Exp (Warsz)* 50: 95–104, 2002.
13. **Bottini N, Stefanini L, Williams S, Alonso A, Jascur T, Abraham RT, Couture C, Mustelin T.** Activation of ZAP-70 through specific dephosphorylation at the inhibitory Tyr-292 by the low molecular weight phosphotyrosine phosphatase (LMPTP). *J Biol Chem* 277: 24220–24224, 2002.
14. **Brazma A, Hingamp P, Quackenbush J, Sherlock G, Spellman P, Stoeckert C, Aach J, Ansorge W, Ball CA, Causton HC, Gaasterland T, Glenisson P, Holstege FC, Kim IF, Markowitz V, Matese JC, Parkinson H, Robinson A, Sarkans U, Schulze-Kremer S, Stewart J, Taylor R, Vilo J, Vingron M.** Minimum information about a microarray experiment (MIAME)-toward standards for microarray data. *Nat Genet* 29: 365–371, 2001.
15. **Breitling R, Li Y, Tesson BM, Fu J, Wu C, Wiltshire T, Gerrits A, Bystrykh LV, de Haan G, Su AI, Jansen RC.** Genetical genomics: spotlight on QTL hotspots. *PLoS Genet* 4: e1000232, 2008.
16. **Broman KW, Wu H, Sen S, Churchill GA.** R/qtl: QTL mapping in experimental crosses. *Bioinformatics* 19: 889–890, 2003.
17. **Bucciantini M, Chiarugi P, Cirri P, Taddei L, Stefani M, Raugei G, Nordlund P, Ramponi G.** The low Mr phosphotyrosine protein phosphatase behaves differently when phosphorylated at Tyr131 or Tyr132 by Src kinase. *FEBS Lett* 456: 73–78, 1999.
18. **Buono C, Binder CJ, Stavrakis G, Witztum JL, Glimcher LH, Lichtman AH.** T-bet deficiency reduces atherosclerosis and alters plaque antigen-specific immune responses. *Proc Natl Acad Sci USA* 102: 1596–1601, 2005.
19. **Busslinger M, Nutt SL, Rolink AG.** Lineage commitment in lymphopoiesis. *Curr Opin Immunol* 12: 151–158, 2000.
20. **Cady FM, O'Neill BP, Law ME, Decker PA, Kurtz DM, Giannini C, Porter AB, Kurtin PJ, Johnston PB, Dogan A, Remstein ED.** Del(6)(q22) and BCL6 rearrangements in primary CNS lymphoma are indicators of an aggressive clinical course. *J Clin Oncol* 26: 4814–4819, 2008.
21. **Chen J, Harrison DE.** Quantitative trait loci regulating relative lymphocyte proportions in mouse peripheral blood. *Blood* 99: 561–566, 2002.
22. **Chesler EJ, Langston MA.** Combinatorial genetic regulatory network analysis tools for high throughput transcriptomic data. In: *Systems Biology and Regulatory Genomics*, edited by Eskin E. Springer, 2006, p. 150–165.
23. **Chesler EJ, Miller DR, Branstetter LR, Galloway LD, Jackson BL, Philip VM, Voy BH, Culiat CT, Threadgill DW, Williams RW, Churchill GA, Johnson DK, Manly KF.** The Collaborative Cross at Oak Ridge National Laboratory: developing a powerful resource for systems genetics. *Mamm Genome* 19: 382–389, 2008.
24. **Churchill GA, Doerge RW.** Empirical threshold values for quantitative trait mapping. *Genetics* 138: 963–971, 1994.
25. **Clementi M, Forabosco P, Amadori A, Zamarchi R, De Silvestro G, Di Gianantonio E, Chieco-Bianchi L, Tenconi R.** CD4 and CD8 T lymphocyte inheritance. Evidence for major autosomal recessive genes. *Hum Genet* 105: 337–342, 1999.
26. **Cope AP, Schulze-Koops H, Aringer M.** The central role of T cells in rheumatoid arthritis. *Clin Exp Rheumatol* 25: S4–11, 2007.
27. **Davies MN, Lawn S, Whatley S, Fernandes C, Williams RW, Schalkwyk LC.** Is blood a reasonable surrogate for brain in gene expression studies? *GeneNetwork* Accession: GN277. http://www.genenetwork.org (January 7, 2010).
28. **Dendrou CA, Plagnol V, Fung E, Yang JH, Downes K, Cooper JD, Nutland S, Coleman G, Himsworth M, Hardy M, Burren O, Healy B, Walker NM, Koch K, Ouwehand WH, Bradley JR, Wareham NJ, Todd JA, Wicker LS.** Cell-specific protein phenotypes for the autoimmune locus IL2RA using a genotype-selectable human bioresource. *Nat Genet* 41: 1011–1015, 2009.

Downloaded from http://physiolgenomics.physiology.org/ by 10.220.32.247 on October 21, 2016

29. **Doss S, Schadt EE, Drake TA, Lusis AJ.** Cis-acting expression quantitative trait loci in mice. *Genome Res* 15: 681–691, 2005.
30. **Du P, Kibbe WA, Lin SM.** lumi: a pipeline for processing Illumina microarray. *Bioinformatics* 24: 1547–1548, 2008.
31. **Fekete A, Soos L, Szekanecz Z, Szabo Z, Szodoray P, Barath S, Lakos G.** Disturbances in B- and T-cell homeostasis in rheumatoid arthritis: suggested relationships with antigen-driven immune responses. *J Autoimmun* 29: 154–163, 2007.
32. **Gentleman RC, Carey VJ, Bates DM, Bolstad B, Dettling M, Dudoit S, Ellis B, Gautier L, Ge Y, Gentry J, Hornik K, Hothorn T, Huber W, Iacus S, Irizarry R, Leisch F, Li C, Maechler M, Rossini AJ, Sawitzki G, Smith C, Smyth G, Tierney L, Yang JY, Zhang J.** Bioconductor: open software development for computational biology and bioinformatics. *Genome Biol* 5: R80, 2004.
33. **Giannoni E, Chiarugi P, Cozzi G, Magnelli L, Taddei ML, Fiaschi T, Buricchi F, Raugei G, Ramponi G.** Lymphocyte function-associated antigen-1-mediated T cell adhesion is impaired by low molecular weight phosphotyrosine phosphatase-dependent inhibition of FAK activity. *J Biol Chem* 278: 36763–36776, 2003.
34. **Giannoni E, Raugei G, Chiarugi P, Ramponi G.** A novel redox-based switch: LMW-PTP oxidation enhances Grb2 binding and leads to ERK activation. *Biochem Biophys Res Commun* 348: 367–373, 2006.
35. **Hemmer B, Archelos JJ, Hartung HP.** New concepts in the immunopathogenesis of multiple sclerosis. *Nat Rev Neurosci* 3: 291–301, 2002.
36. **Hevener AL, Febbraio MA.** The 2009 Stock Conference Report: Inflammation, Obesity and Metabolic Disease. *Obes Rev* 2009.
37. **Huang da W, Sherman BT, Lempicki RA.** Systematic and integrative analysis of large gene lists using DAVID bioinformatics resources. *Nat Protoc* 4: 44–57, 2009.
38. **Jansen RC, Nap JP.** Genetical genomics: the added value from segregation. *Trends Genet* 17: 388–391, 2001.
39. **Kolls JK, Linden A.** Interleukin-17 family members and inflammation. *Immunity* 21: 467–476, 2004.
40. **Kose H, Sakai T, Tsukumo S, Wei K, Yamada T, Yasutomo K, Matsumoto K.** Maturational arrest of thymocyte development is caused by a deletion in the receptor-like protein tyrosine phosphatase kappa gene in LEC rats. *Genomics* 89: 673–677, 2007.
41. **Kraal G, Weissman IL, Butcher EC.** Genetic control of T-cell subset representation in inbred mice. *Immunogenetics* 18: 585–592, 1983.
42. **Lander E, Kruglyak L.** Genetic dissection of complex traits: guidelines for interpreting and reporting linkage results. *Nat Genet* 11: 241–247, 1995.
43. **Langston MA, Perkins AD, Saxton AM, Scharff JA, Voy BH.** Innovative computational methods for transcriptomic data analysis: A case study in the use of FPT for practical algorithm design and implementation. *Comput J* 51: 26–38, 2008.
44. **Leipe J, Skapenko A, Lipsky PE, Schulze-Koops H.** Regulatory T cells in rheumatoid arthritis. *Arthriris Res Ther* 7: 93, 2005.
45. **Lu L, Wei L, Peirce JL, Wang X, Zhou J, Homayouni R, Williams RW, Airey DC.** Using gene expression databases for classical trait QTL candidate gene discovery in the BXD recombinant inbred genetic reference population: mouse forebrain weight. *BMC Genomics* 9: 444, 2008.
46. **Maatta M, Liakka A, Salo S, Tasanen K, Bruckner-Tuderman L, Autio-Harmainen H.** Differential expression of basement membrane components in lymphatic tissues. *J Histochem Cytochem* 52: 1073–1081, 2004.
47. **MacDonell KB, Chmiel JS, Poggensee L, Wu S, Phair JP.** Predicting progression to AIDS: combined usefulness of CD4 lymphocyte counts and p24 antigenemia. *Am J Med* 89: 706–712, 1990.
48. **Malentacchi F, Marzocchini R, Gelmini S, Orlando C, Serio M, Ramponi G, Raugei G.** Up-regulated expression of low molecular weight protein tyrosine phosphatases in different human cancers. *Biochem Biophys Res Commun* 334: 875–883, 2005.
49. **Martinuzzi E, Lemonnier FA, Boitard C, Mallone R.** Measurement of CD8 T cell responses in human type 1 diabetes. *Ann NY Acad Sci* 1150: 61–67, 2008.
50. **Marzocchini R, Malentacchi F, Biagini M, Cirelli D, Luceri C, Caderni G, Raugei G.** The expression of low molecular weight protein tyrosine phosphatase is up-regulated in 1,2-dimethylhydrazine-induced colon tumours in rats. *Int J Cancer* 122: 1675–1678, 2008.
51. **Miyairi I, Tatireddigari VR, Mahdi OS, Rose LA, Belland RJ, Lu L, Williams RW, Byrne GI.** The p47 GTPases Iigp2 and Irgb10 regulate innate immunity and inflammation to murine Chlamydia psittaci infection. *J Immunol* 179: 1814–1824, 2007.
52. **Myrick C, DiGuisto R, DeWolfe J, Bowen E, Kappler J, Marrack P, Wakeland EK.** Linkage analysis of variations in CD4:CD8 T cell subsets between C57BL/6 and DBA/2. *Genes Immun* 3: 144–150, 2002.
53. **Nakamura M, Kishi M, Sakaki T, Hashimoto H, Nakase H, Shimada K, Ishida E, Konishi N.** Novel tumor suppressor loci on 6q22–23 in primary central nervous system lymphomas. *Cancer Res* 63: 737–741, 2003.
54. **Nishimura S, Manabe I, Nagasaki M, Eto K, Yamashita H, Ohsugi M, Otsu M, Hara K, Ueki K, Sugiura S, Yoshimura K, Kadowaki T, Nagai R.** CD8+ effector T cells contribute to macrophage recruitment and adipose tissue inflammation in obesity. *Nat Med* 15: 914–920, 2009.
55. **Passador-Gurgel G, Hsieh WP, Hunt P, Deighton N, Gibson G.** Quantitative trait transcripts for nicotine resistance in Drosophila melanogaster. *Nat Genet* 39: 264–268, 2007.
56. **Peirce JL, Lu L, Gu J, Silver LM, Williams RW.** A new set of BXD recombinant inbred lines from advanced intercross populations in mice. *BMC Genet* 5: 7, 2004.
57. **Petkova SB, Yuan R, Tsaih SW, Schott W, Roopenian DC, Paigen B.** Genetic influence on immune phenotype revealed strain-specific variations in peripheral blood lineages. *Mouse Phenome Database Project*: Petkova1. The Jackson Laboratory. http://www.jax.org/phenome (January 7, 2010).
58. **Philip VM, Duvvuru S, Gomero B, Ansah TA, Blaha CD, Cook MN, Hamre KM, Lariviere WR, Matthews DB, Mittleman G, Goldowitz D, Chesler EJ.** High-throughput behavioral phenotyping in the expanded panel of BXD recombinant inbred strains. *Genes Brain Behav* 2009 Sep 22 [Epub ahead of print].
59. **Schadt EE, Monks SA, Drake TA, Lusis AJ, Che N, Colinayo V, Ruff TG, Milligan SB, Lamb JR, Cavet G, Linsley PS, Mao M, Stoughton RB, Friend SH.** Genetics of gene expression surveyed in maize, mouse and man. *Nature* 422: 297–302, 2003.
60. **Sen S, Churchill GA.** A statistical framework for quantitative trait mapping. *Genetics* 159: 371–387, 2001.
61. **Sethu S, Mendez-Corao G, Melendez AJ.** Phospholipase D1 plays a key role in TNF-alpha signaling. *J Immunol* 180: 6027–6034, 2008.
62. **Shifman S, Bell JT, Copley RR, Taylor MS, Williams RW, Mott R, Flint J.** A high-resolution single nucleotide polymorphism genetic map of the mouse genome. *PLoS Biol* 4: e395, 2006.
63. **Skapenko A, Leipe J, Lipsky PE, Schulze-Koops H.** The role of the T cell in autoimmune inflammation. *Arthritis Res Ther* 7, *Suppl* 2: S4–S14, 2005.
64. **Souza AC, Azoubel S, Queiroz KC, Peppelenbosch MP, Ferreira CV.** From immune response to cancer: a spot on the low molecular weight protein tyrosine phosphatase. *Cell Mol Life Sci* 66: 1140–1153, 2009.
65. **Spina C, Saccucci P, Bottini E, Gloria-Bottini F.** ACP1 genetic polymorphism and colon cancer. *Cancer Genet Cytogenet* 186: 61–62, 2008.
66. **Starr TK, Allaei R, Silverstein KA, Staggs RA, Sarver AL, Bergemann TL, Gupta M, O'Sullivan MG, Matise I, Dupuy AJ, Collier LS, Powers S, Oberg AL, Asmann YW, Thibodeau SN, Tessarollo L, Copeland NG, Jenkins NA, Cormier RT, Largaespada DA.** A transposon-based genetic screen in mice identifies genes altered in colorectal cancer. *Science* 323: 1747–1750, 2009.
67. **Storey JD, Tibshirani R.** Statistical significance for genomewide studies. *Proc Natl Acad Sci USA* 100: 9440–9445, 2003.
68. **Tada Y, Ho A, Koh DR, Mak TW.** Collagen-induced arthritis in CD4- or CD8-deficient mice: CD8+ T cells play a role in initiation and regulate recovery phase of collagen-induced arthritis. *J Immunol* 156: 4520–4526, 1996.
69. **Tailor P, Gilman J, Williams S, Couture C, Mustelin T.** Regulation of the low molecular weight phosphotyrosine phosphatase by phosphorylation at tyrosines 131 and 132. *J Biol Chem* 272: 5371–5374, 1997.
70. **Tanigaki K, Honjo T.** Regulation of lymphocyte development by Notch signaling. *Nat Immunol* 8: 451–456, 2007.
71. **Taylor BA, Bedigian HG, Meier H.** Genetic studies of the Fv-1 locus of mice: linkage with Gpd-1 in recombinant inbred lines. *J Virol* 23: 106–109, 1977.
72. **Taylor BA, Wnek C, Kotlus BS, Roemer N, MacTaggart T, Phillips SJ.** Genotyping new BXD recombinant inbred mouse strains and comparison of BXD and consensus maps. *Mamm Genome* 10: 335–348, 1999.
73. **Tripp RA, Hou S, McMickle A, Houston J, Doherty PC.** Recruitment and proliferation of CD8+ T cells in respiratory virus infections. *J Immunol* 154: 6013–6021, 1995.

Downloaded from http://physiolgenomics.physiology.org/ by 10.220.32.247 on October 21, 2016

74. **Van Meerwijk JP, Bianchi T, Marguerat S, MacDonald HR.** Thymic lineage commitment rather than selection causes genetic variations in size of CD4 and CD8 compartments. *J Immunol* 160: 3649–3654, 1998.
75. **Vercauteren SM, Sutherland HJ.** Constitutively active Notch4 promotes early human hematopoietic progenitor cell maintenance while inhibiting differentiation and causes lymphoid abnormalities in vivo. *Blood* 104: 2315–2322, 2004.
76. **Voy BH, Scharff JA, Perkins AD, Saxton AM, Borate B, Chesler EJ, Branstetter LK, Langston MA.** Extracting gene networks for low-dose radiation using graph theoretical algorithms. *PLoS Comput Biol* 2: e89, 2006.
77. **Wang SE, Wu FY, Shin I, Qu S, Arteaga CL.** Transforming growth factor β (TGF-β)-Smad target gene protein tyrosine phosphatase receptor type kappa is required for TGF-β function. *Mol Cell Biol* 25: 4703–4715, 2005.
78. **Weisberg SP, Hunter D, Huber R, Lemieux J, Slaymaker S, Vaddi K, Charo I, Leibel RL, Ferrante AW Jr.** CCR2 modulates inflammatory and metabolic effects of high-fat feeding. *J Clin Invest* 116: 115–124, 2006.
79. **Xu Y, Shao Y, Voorhees JJ, Fisher GJ.** Oxidative inhibition of receptor-type protein-tyrosine phosphatase kappa by ultraviolet irradiation activates epidermal growth factor receptor in human keratinocytes. *J Biol Chem* 281: 27389–27397, 2006.
80. **Yamada H, Nakashima Y, Okazaki K, Mawatari T, Fukushi JI, Kaibara N, Hori A, Iwamoto Y, Yoshikai Y.** Th1 but not Th17 cells predominate in the joints of patients with rheumatoid arthritis. *Ann Rheum Dis* 67: 1299–1304, 2008.
81. **Yang Y, Gil MC, Choi EY, Park SH, Pyun KH, Ha H.** Molecular cloning and chromosomal localization of a human gene homologous to the murine R-PTP-kappa, a receptor-type protein tyrosine phosphatase. *Gene* 186: 77–82, 1997.
82. **Yasukawa K, Oshiumi H, Takeda M, Ishihara N, Yanagi Y, Seya T, Kawabata S, Koshiba T.** Mitofusin 2 inhibits mitochondrial antiviral signaling. *Sci Signal* 2: ra47, 2009.
83. **Ye Q, Shieh JH, Morrone G, Moore MA.** Expression of constitutively active Notch4 (Int-3) modulates myeloid proliferation and differentiation and promotes expansion of hematopoietic progenitors. *Leukemia* 18: 777–787, 2004.
84. **Zhang Y, Chesler EJ, Langston MA.** On Finding bicliques in bipartite graphs: a novel algorithm with application to the integration of diverse biological data types. In: *Proceedings, Hawai'i International Conference on System Sciences*. Big Island, HI: 2008.
85. **Zhang Y, Siebert R, Matthiesen P, Yang Y, Ha H, Schlegelberger B.** Cytogenetical assignment and physical mapping of the human R-PTP-kappa gene (PTPRK) to the putative tumor suppressor gene region 6q22.2-q223. *Genomics* 51: 309–311, 1998.
86. **Zhang ZL, Constantinou D, Mandel TE, Georgiou HM.** Lymphocyte subsets in thymus and peripheral lymphoid tissues of aging and diabetic NOD mice. *Autoimmunity* 17: 41–48, 1994.

Downloaded from http://physiolgenomics.physiology.org/ by 10.220.32.247 on October 21, 2016